Catal Lett (2009) 128:290–296
DOI 10.1007/s10562-008-9714-z

1-Hexene Double Bond Isomerization Reaction Over $SO_4^=$ Promoted NiO, Al_2O_3 and ZrO_2 Acid Catalysts

M. Pérez-Luna · A. Cosultchi · J. A. Toledo-Antonio · L. Díaz-Garcia

Received: 11 June 2008 / Accepted: 26 September 2008 / Published online: 11 November 2008

Abstract Sulfated mixed oxides, $SO_4^=$/Ni–Al–O and $SO_4^=$/Zr–Al–O were evaluated for double bond isomerization (DBI) of 1-hexene using helium and hydrogen as carrier gases. The increase of temperature from 100 to 200 °C seems to favor the deprotonation pathway and contribute to increase the 1-hexene conversion for both catalysts and without regard of the carrier gas. The results indicate that temperature it is the main factor that contributes to improve both conversion and selectivity towards (*cis* + *trans*)-2-hexene, while the reductive atmosphere beneficiate only the $SO_4^=$/Ni–Al–O catalyst performance, as hydrogen prevents this catalyst from a fast deactivation.

Keywords Double bond isomerization · Olefin isomerization · Sulfated mixed oxides

1 Introduction

The recent developed Gas to Liquid process, yield gasoline by Fisher Tropsch type synthesis, with high olefinic compounds, which bring about a renovate interest in the olefin isomerization process, by means octane number can be increased by twice the original value [1]. Recent studies demonstrate that shifting the C=C double bond from a terminal position to an internal position, FCC gasoline can preserve their olefinic compounds and boost the octane number even after a highly hydrogenating conditions of the HDS process [2].

α-olefins are linear alkenes with a double bond at the terminal position. Double-bond isomerization (DBI) of such olefins implicates migration or shifting of the double-bond along the carbon chain and *cis-trans* rearrangement. Apparently, the double-bond shift reaction (DBS) is faster than skeletal rearrangement since it involves the migration of only one hydrogen atom instead of an alkyl group. Additionally, a series of other complex reactions such as disproportionation, cyclization, polymerization, oligomerization and cracking, may occur alongside with DBI reaction [3–10]. Catalyst type and operational temperature are key factors for the selectivity of DBI reaction, while an increase of the catalyst acidity contributes to raise the yield of side products [11]. For example, thermodynamic and kinetic aspects of 1-pentene isomerization reaction over ZMS-5 suggest that oligomerization and cracking products appear at temperatures as high as 250 °C, whereas skeletal rearrangement reaches a maximum yield between 250 and 300 °C [12].

Resofszki et al. [13] indicate that, DBI reaction is an intramolecular reaction, although, hydrogen uptake from the acidic surface is not negligible and olefin interaction with an acidic substrate starts with the coordination of the double-bond to the metal ion of transition metal oxides. The catalytic activity was correlated with the electronegativity and the number of d electrons of the metal.

Abbot et al. [14] assume that the mechanism of DBI reaction is an ionic mechanism on both acidic and basic catalysts, while previously, other authors indicated that such reaction is an acid-catalyzed reaction which involves mainly the Brönsted sites of relatively low acid strength [15]. However, reactions other than DBI as olefins

---

M. Pérez-Luna (✉) · A. Cosultchi · J. A. Toledo-Antonio · L. Díaz-Garcia
Instituto Mexicano del Petroleo, Eje Central Lázaro Cárdenas # 152, 07730 Mexico, D.F., Mexico
e-mail: mperezl@imp.mx

M. Pérez-Luna
Department of Metallurgical Engineering-ESIQIE, Instituto Politécnico Nacional, Zacatenco 07738 Mexico, D.F., Mexico

dimerization are also stimulated by a high acidity regardless the type of substrate [16].

With acid catalysts, DBI reaction of α-olefins may proceed as a consecutive-parallel reaction starting with a proton addition from the substrate to the terminal double-bond with the formation of carbenium ion followed by proton elimination [13, 15, 17, 18], or with the formation of a π-allylic intermediate when all isomers appear at the start of the reaction [19, 20].

Most transition metals metal oxides or metallocene alkyne complexes are capable to catalyze DBI reactions [4, 7–9] as well as alumina as catalyst treated with HCl or as support shows a high yielding rate for DBS reaction [10]. Additionally, based on reaction mechanism, it is expected that sulfate metal oxides would also catalyze DBI reactions, although, other reactions such as oligomerization or cracking require also catalysts with strong acid sites [3, 21].

A sulfated metal oxide is a solid superacid catalyst which bears strong acid sites on its surface. The high activity of these catalysts has been related to the presence of both Brönsted and Lewis acidic sites on the surface [22, 23]. The structure and physicochemical properties of the catalyst depend on the metal oxide and sulfate and its interaction with the selected support. For example, alumina is adequate support to improve the thermal stability of the catalyst without modification of its acidic character.

The sulfate species play a dual role, as a source of higher acidity, providing the proton involves in isomerization mechanism [24] and an oxidizing character exerting an induction effect on nickel or zirconia metals and on the hydration factor of the sulfate species formed after calcination.

Sulfated metal oxides catalysts such as $SO_4^=/NiO–SiO_2$ and $SO_4^=/ZrO_2–Al_2O_3$ has already proved their efficiency for hydrocarbon skeletal isomerization and cracking reactions [9, 25]. Nickel compounds supported on oxides as nickel sulfate has been used for dimerization and oligomerization of olefins and its activity is related to the acidic property of the surface and to the low oxidation state Ni ions [16].

The use of hydrogen as carrier gas was proposed as a mean to provide the adequate amount of protons to the DBI reaction and as a mechanism to control reaction selectivity and avoid undesirable side reactions [26, 27]. In this work, two catalysts: $SO_4^=/ZrO_2–Al_2O_3$ and $SO_4^=/NiO–Al_2O_3$, were tested for α-hexene DBI reaction at temperatures from 100 to 200 °C. The catalytic activity of both sulfated solid catalysts was tested in a reduced atmosphere and compared to their activity in an inert atmosphere by using hydrogen and helium, respectively, as carrier gases. Additionally, zirconia and nickel oxides supported on alumina were also tested for the same DBI reaction.

2 Experimental

2.1 Synthesis of Materials

The nickel-alumina promoted catalyst, Ni–Al–O, was prepared by co-precipitation of $Ni(NO_3)_2$ $6H_2O$ and $Al(NO_3)_3$ $9H_2O$, (Aldrich 99.9 wt%) with a 15 wt% of NH_4OH (J. T. Baker) solution, added drop by drop until a pH of 8.5 is reached. The precipitate cake was washed and filtered repeatedly with deionized water. Thereafter the clean filtrated cake was dried at 110 °C and heated at 650 °C at a 5 °C/min rate and maintained at this temperature during 4 h.

The zirconium-alumina promoted catalyst, Zr–Al–O, was prepared in similar way by using $ZrO(NO_3)_2$ $6H_2O$ and $Al(NO_3)_3$ $9H_2O$, (Aldrich 99.9 wt%) as co-precipitants. The sulfated catalysts were prepared starting from the previously filtrated and dried cakes at 110 °C; a fraction of both dried cakes were impregnated by incipient wetness with a 3 M H_2SO_4 solution at room temperature and further dried at 110 °C; and annealed at 650 °C in air for 4 h.

2.2 Characterization Techniques

The chemical composition was determined by Atomic Absorption Spectroscopy (AAS) in a Perkin Elmer S-2380 apparatus; the amount of sulfur was determined by combustion in a LECO SC-44 apparatus. Specific surface area measurements were carried out in a Micromeritics Digisorb 2600 apparatus according to ASTM-D-3663.

The total acidity was measured by NH_3 titration in an Altamira AMI 2000 equipped with a thermal conductivity detector (TCD). 200 mg of sample was pretreated under flowing N_2 at 500 °C for 4 h. Then, the sample was cooled down to 150 °C and, calibrated pulses of NH_3 were injected through a 6 port on-line valve until saturation of the sample was reached. The amount of NH_3 adsorbed by the sample was calculated from the difference between the total amount of NH_3 injected and the amount of NH_3 calculated from the TCD signals.

2.3 Catalytic Activity

The 1-hexene isomerization reactions were run at atmospheric pressure and at three temperatures: 100, 150 and 200 °C; using, separately, He and H_2 as carrier gases at 10 mL/min. The WSHV was 2.076 h^{-1} and the maximum time-on-stream was 5 h. The reaction was carried out in a stainless-steel fixed bed micro reactor (7 mm of diameter, 150 mm of length), using 1-hexene (Aldrich 99 wt%) as olefin feed and 0.3 g of powdered catalyst samples previously treated under air flow (30 cm^3/min) at 500 °C for 1 h.

The reaction products were analyzed on-line by using a Hewlett-Packard 5890 Gas Chromatograph coupled with a flame ionization detector. The chromatographic column used was a 5 m × 1/8″ silicone gum rubber SE-30 on Cromosorb-W glass capillary column. During the analysis the column temperature was controlled at 125 °C. The main products observed were the expected linear olefinic structures: 1-, 2- and 3-hexene.

In order to evaluate the effect of temperature on 1-hexene DBI, the reaction was run without catalysts between 100 and 250 °C. At such conditions, no reaction products were detected.

3 Results

3.1 Textural, Structural and, Acid Properties of the Catalysts

Table 1 shows chemical composition of the catalysts determined by atomic absorption spectroscopy. The results show that NiO and ZrO_2 were added nearly at the same proportion to obtain a mixed oxide with Al_2O_3. Additionally, both catalysts contain a similar amount of H_2SO_4, although, they show different acidity, measured as the amount of adsorbed ammonium per gram of catalyst. For unsulfated samples the BET area stands around 200 m^2/g and decreases slightly for the corresponding sulfated catalysts. The mean pore diameters are higher for SO_4/Ni–Al–O than for SO_4/Zr–Al–O catalysts.

It is interesting to note that even if the unsulfated Ni–Al–O sample exhibited a higher acidity than the sulfated catalysts samples (see Table 1), none of the unsulfated catalysts, Zr–Al–O or Ni–Al–O, show any catalytic activity for DBI reaction at the operational conditions.

3.2 Catalytic Activity

Table 2 shows the conversion and selectivity data taken at the steady state conditions after 300 min time on stream (TOS) for the corresponding sulfated samples, $SO_4^=$/Ni–Al–O and $SO_4^=$/Zr–Al–O, evaluated in inert and reducing atmosphere.

Catalytic activity improved with the reaction temperature in both inert and reducing atmosphere. For both sulfated catalysts, the selectivity towards (*cis* + *trans*)-2-hexene increased with temperature in both atmospheres. However, at low temperature, 100 °C, only $SO_4^=$/Ni–Al–O catalyst shown certain selectivity towards (*cis* + *trans*)-3-

Table 1 Chemical composition and textural characteristics of tested catalysts

Catalyst	Composition (wt %)				BET area $(m^2\ g^1)$	Mean pore diameter (Å)	Pore volume, $(cm^3\ g^{-1})$	Acidity Meq $(NH_3)\ (g^{-1})$
	NiO	ZrO_2	Al_2O_3	H_2SO_4				
Ni–Al–O	23.73		76.27		199.8	60	0.30	0.3675
$SO_4^=$/Ni–Al–O	21.80		64.20	13.97	179.0	63	0.28	0.6528
Zr–Al–O		28.85	71.15		211.0	53	0.28	0.1234
$SO_4^=$/Zr–Al–O		25.11	61.36	13.53	205.1	48	0.25	0.3339

Table 2 Catalytic activity[a] of sulfated catalysts during 1-hexene double bond shifting reaction in H_2 and He atmosphere, at different temperatures

Catalyst	Carrier	Temperature (°C)	Conversion (mol %)	Selectivity (mol %)	
				2-Hexene	3-Hexene
$SO_4^=$/Ni–Al–O	He	100	7.4	50	50
	He	150	64	62	38
	He	200	92	73	27
	H_2	100	9.2	45	55
	H_2	150	72	62	38
	H_2	200	91	72	28
$SO_4^=$/Zr–Al–O	He	100	23	56	44
	He	150	52	61	39
	He	200	73	67	33
	H_2	100	19	82	18
	H_2	150	46	65	35
	H_2	200	67	66	34

[a] Conversion and selectivity data taken at the steady state reaction after 300 min time on stream

hexene and in both atmospheres. On the contrary, the reaction selectivity towards (*cis* + *trans*)-2-hexene is similar for $SO_4^=$/Zr–Al–O catalyst at any temperature and in any atmosphere.

The deactivation profiles of 1-hexene conversion with TOS, in inert and reducing atmosphere, for both sulfated catalysts are presented in Figs. 1 and 2. As reaction temperature increases, the 1-hexene conversion also increases, for both catalysts and for both carrier gases. At low temperature, 100 °C, the $SO_4^=$/Zr–Al–O catalyst shows higher catalytic activity than that of $SO_4^=$/Ni–Al–O. However, $SO_4^=$/Zr–Al–O strongly deactivates with TOS and mainly in reductive atmosphere (see Fig. 1).On the contrary, the catalytic activity is more stable for $SO_4^=$/Ni–Al–O catalyst, especially in reductive atmosphere and its deactivation, as a consequence of TOS, is more pronounced at low temperature and in inert atmosphere.

Generally, both catalysts favored the formation of (*cis* + *trans*)-2-hexene as primary product for temperatures beyond 150 °C. At lower temperature, 100 °C, (*cis* + *trans*)-3-hexene was favored on $SO_4^=$/Ni–Al–O catalyst, in both He and H_2 atmosphere, whereas on $SO_4^=$/Zr–Al–O catalyst (*cis* + *trans*) 2-hexene was the main product. Additionally, no skeletal isometization products were detected at the all experimental conditions.

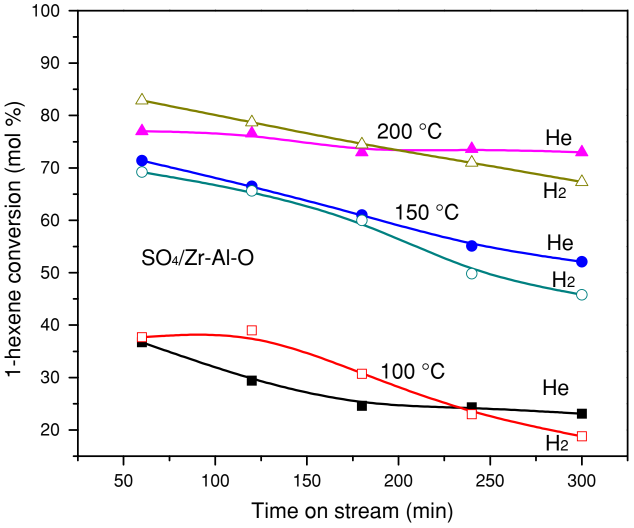

Fig. 1 Deactivation profile of $SO_4^=$/Zr–Al–O catalyst during 1-hexene conversion in He and H_2 atmospheres, as indicated

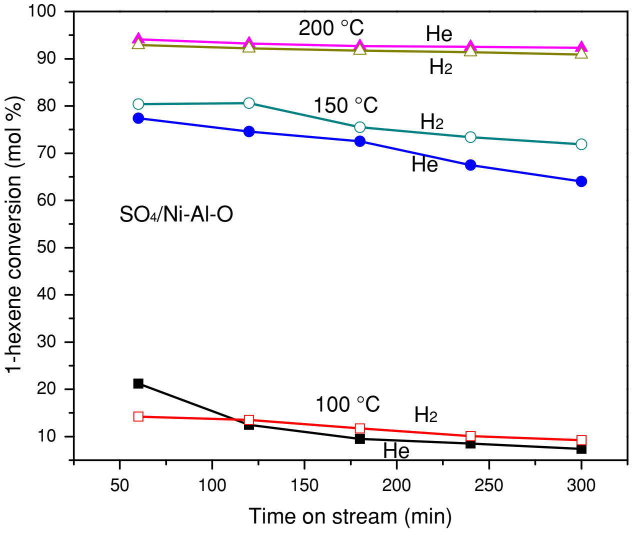

Fig. 2 Deactivation profile of $SO_4^=$/Ni–Al–O catalyst during 1-hexene conversion in He and H_2 atmospheres, as indicated

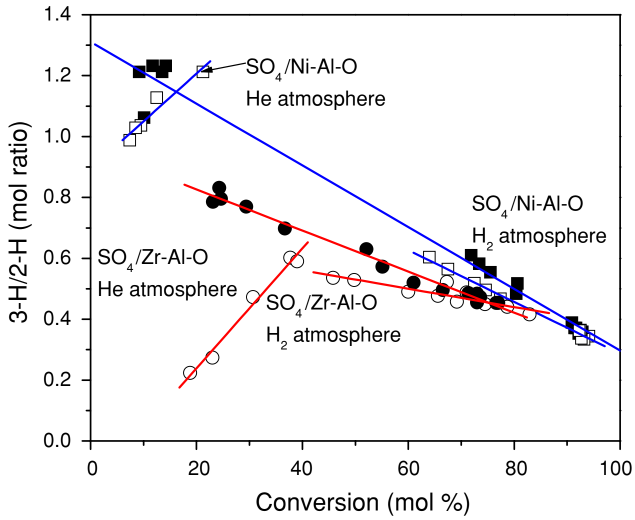

Fig. 3 Ratio of 3-hexene to 2-hexene as a function of 1-hexene conversion for both $SO_4^=$/Ni–Al–O and $SO_4^=$/Zr–Al–O catalysts. (■ $SO_4^=$/Ni–Al–O in H_2; □ $SO_4^=$/Ni–Al–O in He; ● $SO_4^=$/Zr–Al–O in He; ○ $SO_4^=$/Zr–Al–O in H_2)

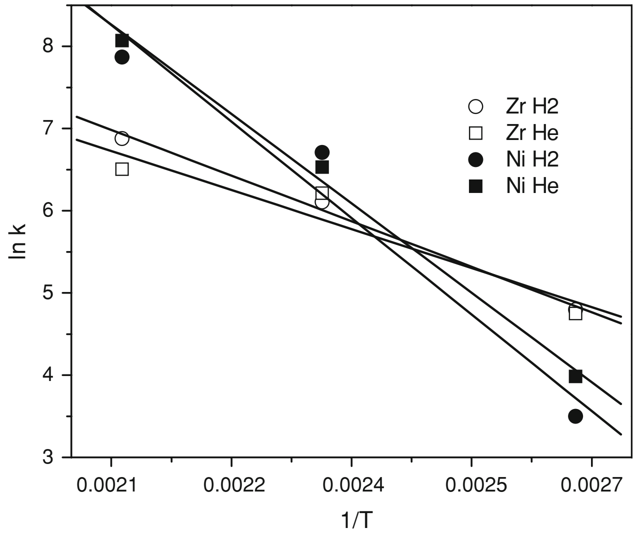

Fig. 4 Arrhenius equation plots used to calculate the activation energy of 1-hexene DBS reaction

The ratio of the selectivity product: (*cis* + *trans*)-3-hexene/(*cis* + *trans*)-2-hexene (3-H/2-H ratio) was plotted as a function of 1-hexene conversion and presented in Fig. 3, for both atmospheres.

For $SO_4^=$/Ni–Al–O catalyst the 3-H/2-H ratio is higher than 1.0 for both atmospheres but only at low conversion level, which corresponds to low reaction temperature of 100 °C. As the 1-hexene conversion increases, this ratio decreases independently on the carrier gas, approximating to a 3-H/2-H ratio value around 0.3 to 0.2 at 200 °C.

For $SO_4^=$/Zr–Al–O catalyst, the 3-H/2-H ratio increases from 0.2 to 0.6 but only in H_2 atmosphere at a conversion as high as 40 mol %. For this catalyst, even the reaction develops at higher temperatures, this ratio stills similar.

Figure 4 shows the thermal behavior of the tested catalysts. The activation energy for each reaction presented in Table 3 was obtained from this plot. The $SO_4^=$/Zr–Al–O catalyst has the smallest activation energy when He are used as carrier gas.

4 Discussion

The catalytic activity of solid acid catalysts has been correlated with a series of features such as: metal electronegativity, nature of the binder material, intrinsic sulfate group content, coordination state of oxygen and sulfur in the catalyst, etc.

The catalytic activity of oxides is normally correlated to the metal electronegativity and the corresponding number of *d*-electrons [13] or coordination number of metal cation. Electronegativity for Ni, is 4.4 eV while for Zr, it is 3.64 eV, both in the Mulliken scale. Ni has 8*d*-electrons while Zr has only 2*d*-electrons [28]. However, while the oxidation state of Ni is +2, for Zr can be either, +2, +3 or +4.

Most studies indicate that the high activity of these catalysts for hydrocarbon reactions such as isomerization is related to both Brönsted and Lewis acidic sites on the catalyst surface [15]. However, other authors claim that catalysts such as $SO_4^=$/Zr–Al–O, rather than behaving as superacids, they operate via a one electron oxidation mechanism in which an electron is transferred between the substrate and the sulfate group [29].

Table 3 Activation energy calculated from Fig. 5 plots

Catalyst	Carrier gas	Ea, Activation energy, kJ*mol^{-1}
$SO_4^=$/Ni–Al–O	He	60.26
$SO_4^=$/Ni–Al–O	H_2	65.04
$SO_4^=$/Zr–Al–O	He	26.16
$SO_4^=$/Zr–Al–O	H_2	30.54

Recent studies describe different operating mechanism for sulfated zirconia samples: (i) the active surface sites consists in polysulfate species with mainly three or four S atoms and two ionic bonds of S–O–Zr in addition to S=O coordination bonds with Zr, the active site being Lewis sites on the S atoms [30]; (ii) the active sites are a complex mixture of open trimer with zirconium atoms bonded by sulfate groups while bridge sulfate groups form Zr–O–S–O–Zr bonds; and three terminal sulfate groups and three terminal hydroxyl groups for each zirconium atom [31]. Moreover, Yamaguchi [32] concluded that the generation of high acidity was accompanied by the formation of S^{6+} or S^{7+} species on metal surface and therefore, the electronegativity and coordination number of metal cation in the metal oxide affect the acid strength. For a catalyst such as $SO_4^=$/Ni–Al–O, the active sites responsible for catalytic activity consist of low oxidation state of nickel ions and the higher the acidity, the higher should be the catalytic activity, at least for ethylene dimerization with nickel-containing catalysts [16].

The coordination number for ZrO_2 is reported as 7 and 8, while for NiO it is 6. However, as Table 1 results indicate, the acidity of the tested catalysts, measured as adsorbed ammonium, is lower for $SO_4^=$/Zr–Al–O than for $SO_4^=$/Ni–Al–O, even though both catalysts have nearly the same content of alumina and H_2SO_4. Thus, when $SO_4^=$/Zr–Al–O is used as catalyst for α-hexene isomerization a lower catalytic activity followed by a faster deactivation can be expected, if compared to $SO_4^=$/Ni–Al–O catalyst behavior.

From *ab-initio* calculations of 1-hexene isomerization using aluminosilicate molecular sieve as catalyst, the activation energy is 104.9 kJ/mol [33]. The calculated activation energies reported in Table 3 for both catalysts, $SO_4^=$/Zr–Al–O and $SO_4^=$/Ni–Al–O, and using He and H2 as carrier gases are lower than those reported in [33], but similar to those reported in literature for some deactivated catalyst [34, 35]. Values of 70 kJ/mol and 54 kJ/mol were reported as related to the catalyst deactivation due to pore diffusion limitations [34, 35].

The calculated mean pore diameter for $SO_4^=$/Zr–Al–O catalyst is also lower than that calculated for $SO_4^=$/Ni–Al–O catalyst: 48 Å compared to 63 Å, respectively, as reported in Table 1. Thus, a lower pore diameter could be an indication that the reaction is controlled by pore diffusion process, in a similar way that occurs with zeolite catalysts [14, 34, 35]. Consequently, if the activation energy is lower than expected for such catalysts, it is an indication that DBI reaction pore diffusion limitations are more significant than expected.

With an acid catalyst, a DBI reaction of α-olefins may proceed as a consecutive-parallel reaction starting with a proton addition from the substrate to the terminal double-bond with the formation of carbenium ion followed by proton elimination when 1-hexene converts to *trans*-2-hexene and then to *cis*-2-hexene, followed by (*cis* + *trans*)-3-hexene formation [13, 15, 17, 18]; or if all hexene isomers appear at the same time, the isomerization follows, instead, a π-allylic intermediate formation [19, 20].

A higher acidic strength facilitates hydrogen transfer but also favors paraffin and aromatic formation. On the contrary, olefins are the result of a less hydrogen transfer [36]. However, the use of hydrogen as carrier gas was proposed as a mechanism to provide the desirable concentration of the strong acid sites in order to control the selectivity of the DBI reaction and avoid undesirable side reactions [26, 27].

As the reaction temperature increases there is a rise in the reaction conversion. However, while at 100 °C conversion on $SO_4^=$/Zr–Al–O is higher than for $SO_4^=$/Ni–Al–O, at 150 °C and 200 °C, the opposite occurs.

For $SO_4^=$/Zr–Al–O, the reaction selectivity is displaced towards (*cis* + *trans*)-2-hexene production is similar -the ratio of 3-H/2-H is about 0.6- independently on temperature and a atmosphere.

For $SO_4^=$/Ni–Al–O the selectivity towards (*cis* + *trans*)-2-hexene increases continuously –the ratio of 3-H/2-H diminishes from 1.2 to near 0.35- as the temperature increases and independently on the atmosphere.

As a consequence of time-on stream, a faster declination of 1-hexene conversion is observed for $SO_4^=$/Zr–Al–O catalyst at all tested temperatures without regard of the atmosphere (see Fig. 1). This is probable due to a strong interaction of reactant or product molecules with the acidic sites as well as to its inability to protonate the reactants. On the contrary, for $SO_4^=$/Ni–Al–O catalyst, a similar declination is observed only for He atmosphere (see Fig. 2).

According to theoretical optimum performance envelope (OPE) [37], the curves in Fig. 3 can be interpreted as follows:

(a) For $SO_4^=$/Ni–Al–O catalyst in an inert atmosphere, at low temperature and low conversion, the 3-H/2-H ratio indicate that both isomers (*cis* + *trans*)-2-hexene and (*cis* + *trans*)-3-hexene are stable main products. There is also a tendency to increases the selectivity towards (*cis* + *trans*)-3-hexene.

(b) For $SO_4^=$/Zr–Al–O catalyst at same condition and in a reduced atmosphere, the 3-H/2-H ratios indicates that (*cis* + *trans*)-3-hexene is a secondary stable product.

(c) For both catalysts, at higher temperatures (at 150 and 200 °C), and higher conversions, in both atmospheres, the 3-H/2-H ratios indicates that, (*cis* + *trans*)-3-hexene is an unstable primary product and, consequently, (*cis* + *trans*)-2-hexene is a secondary stable product.

Consequently, depending on catalysts composition and the operational conditions, any of the two mentioned reaction mechanisms could proceed.

Figure 5 a and b show the relative conversion ratio of 1-hexene isomerization in H_2 related to He and calculated as follows: $(x_{H_2}-x_{He})*100/x_{H_2}$ and for both catalysts.

The use of H_2 as carried gas favors the conversion of 1-hexene using $SO_4^=$/Ni–Al–O as catalyst. Moreover, if the relative conversion rate at 100 °C and 60 min TOS is excluded from the plot, it is evident that such conversion

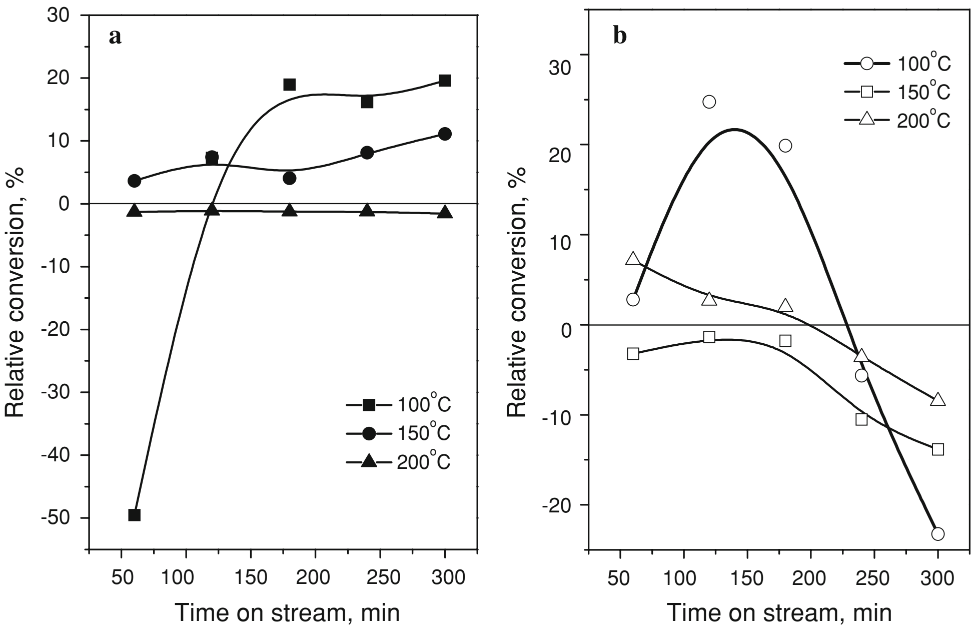

Fig. 5 Relative conversion ration of 1-Hexene in H_2 related to He at 100, 150 and 200 °C for: (**a**) $SO_4^=$/Ni–Al–O; and (**b**) $SO_4^=$/Zr–Al–O catalysts

shows a monotonic decrease related to reaction temperature without any regard to the time on steam. Thus, at lower temperature, 100–150 °C, this catalyst is more sensitive to hydrogen than to helium and the relative conversion increases with the time on stream. This behavior also shows that the effect of H_2 diminishes at higher reaction temperature.

When DBI reaction occurs on $SO_4^=$/Zr–Al–O catalyst, there is no clear evidence of 1-hexene conversion improvement due to the type of atmosphere, neither as a consequence of reaction temperature. Moreover, for this catalyst, the time on stream affects negatively the relative conversion due to the fast catalyst deactivation.

Deactivation of sulfated zirconia catalyst has been already studied and attributed to the reduction of oxidation state of sulfur in the surface complex [38, 39] and also to coke deposition [23]. Nor oligomers nor branched isomers were detected as products of the reaction. Therefore, formation of coke on the zirconia catalyst surface as the main cause of sulfated zirconia deactivation should be eliminated.

In the case of nickel catalyst, the long-term stability could be attributed to the nature of metal. Consequently, there is an improvement of the catalytic stability when hydrogen is used as carrier gas. This is due to the transference of hydrogen atoms to the catalysts surface which regenerates the acid sites after the organic cations were desorbed out of the catalyst surface.

5 Conclusions

The activity of solid acid catalyst for DBI reaction depends on temperature as 1-hexene conversion improves for both catalysts, $SO_4^=$/Ni–Al–O and $SO_4^=$/Zr–Al–O following the increment of the temperature. The reduced atmosphere was beneficial only for $SO_4^=$/Ni–Al–O catalyst as hydrogen maintain the catalyst stability for more TOS. Thus, even though the reduction of the concentration of Lewis acid sites is suppose to be important for this reaction, the use of reduced (H_2) atmosphere did not affect substantially the DBI conversion or selectivity of the tested catalysts.

Consequently, the results indicate that only the temperature contributes to the enhancement of the DBI conversion and selectivity towards (*cis* + *trans*)-2-hexene, while the reductive atmosphere shows no substantial effect on the catalytic selectivity of any of the two catalysts. The effect of temperature on the catalysts performance could be explained as being a consequence of the faster reduction of Lewis acidic sites density, measured as adsorbed pyridine, when the temperature is increased. Consequently, the ratio of Brönsted-to-Lewis acidic sites density increases and, therefore, the desirable effect claimed by Matsuda et al. [26] and Schulz-Ekloff et al. [27] is obtained.

References

1. Dunning HN (1953) Ind & Eng Chem 45:551
2. Toba M, Miki Y, Matsui T, Harada M, Yoshimura Y (2007) Appl Catal A Gen 70:542
3. De Klerk A (2005) Ind Eng Chem Res 44:3887
4. Ohff A, Burlakov VV, Rosenthal U (1996) J Mol Catal A Chem 105:103
5. Cavell KJ, Masters AF (1986) Aust J Chem 39:1129
6. Ayame A, Sawada G (1989) Bull Chem Soc Jpn 62:3055
7. Dallaman K, Buffon R (2001) J Mol Catal A Chem 172:81
8. Chuang JY, Ying L, Ren H (2006) J Mol Catal A Chem 259:17
9. Schmidt B (2006) J Mol Catal A Chem 254:53
10. De Klerk A (2004) Ind Eng Chem Res 43:6325
11. Otremba T, Tanievski M (1980) React Kinet Catal Lett 15(2):279
12. Mäurer T, Kraushaar-Czarnetzki B (1999) J Catal 187:202
13. Resofski G, Gáti G, Hálasz I (1985) Appl Catal 19:241
14. Abbot J, Corma A, Wojciechowski BW (1985) J Catal 92:398
15. Corma A (1995) Chem Rev 95:559
16. Sohn JR, Park WC, Shin DC (2006) J Mol Catal A Chem 256:156
17. Haag WO, Pines H (1960) J Am Chem Soc 82:2488
18. Stepanov AG, Arzumanov SS, Luzgin MV, Ernst H, Freunde D (2005) J Catal 229(1):243
19. Brouwer DM (1962) J Catal 1:22
20. Kokes RJ, Dent AC (1970) Adv Catal 22:1
21. Pater JPG, Jacobs PA, Martens JA (1999) J Catal 184:262
22. Rosenberg DJ, Bachiller-Baeza B, Dimes TJ, Anderson JA (2003) J Phys Chem B 107:6526
23. Hino M, Kobayashi S, Arata K (1979) J Am Chem 101:6439
24. Shimizu K, Kounami N, Wada H, Shishido T, Hattori H (1998) Catal Lett 54:153
25. Perez Luna M, Cosultchi A, Toledo Antonio JA, Arce Estrada EM (2005) Catal Lett 102:33
26. Matsuda T, Fuse T, Kikuchi E (1987) J Catal 106:38
27. Schulz-Ekloff G, Jaeger NI, Vladov C, Petrov L (1987) Appl Catal 33:73
28. Dong YF, Wang SJ, Feng YP, Huan ACH (2006) Phys Rev B 73:045302
29. Farcasiu D, Ghenciu A, Li JQ (1996) J Catal 158:116
30. Hino M, Kurashige M, Matsuhashi H, Arata K (2006) Termochim Acta 44:35
31. Kanazhevskii V, Shmachkova V, Kotsarenko N, Kolomiichuk V, Kochubei D (2006) J Struct Chem 47:860
32. Yamaguchi T (1990) Appl Catal 61:1
33. Pu M, Li Z-H, Gong Y-J, Wu D, Sun Y-H (2003) J Mater Sci Lett 22:955
34. Clark MC, Subramaniam B (1996) Chem Eng Sci 51:2369
35. Clark MC, Subramaniam B (1999) AIChE 45:1559
36. Talukdar AK, Bhattacharyya KG, Baba T, Ono Y (2001) Appl Catal A Gen 213:239
37. Ko AN, Wojciechowski BW (1983) Int J Chem Kinet 15:1249
38. Yori JC, Luy JC, Parera JM (1989) Catl Today 5:493
39. Yori JC, Luy JC, Parera JM (1989) Appl Catal 46:103